Describing the strongly interacting quark-gluon plasma through the Friedberg-Lee model

Song Shu
Faculty of Physics and Electronic Technology, Hubei University, Wuhan 430062, China

Jia-Rong Li
Institute of Particle Physics, Hua-Zhong Normal University, Wuhan 430079, China

(Received 14 July 2010; revised manuscript received 19 September 2010; published 12 October 2010)

The Friedberg-Lee (FL) model is studied at finite temperature and density. The soliton solutions of the FL model in the deconfinement phase transition are solved and thoroughly discussed for certain boundary conditions. We indicate that the solitons before and after the deconfinement have different physical meanings: the soliton before deconfinement represents hadrons, while the soliton after the deconfinement represents the bound state of quarks which leads to a strongly interacting quark-gluon plasma phase. The corresponding phase diagram is given.

DOI: 10.1103/PhysRevC.82.045203 PACS number(s): 25.75.Nq, 12.39.Ki, 11.10.Wx

I. INTRODUCTION

An important discovery at the BNL Relativistic Heavy Ion Collider (RHIC) in recent years is the strongly interacting quark-gluon plasma (sQGP) [1–3]. For the collective effects from RHIC experiments, known as radial and elliptic flow, the QGP could be well described by ideal hydrodynamics. It implies that the QGP at RHIC is the most perfect fluid [4–6]. For this reason, Shuryak has pointed out there should be lots of bound states [1] especially for light and heavy $q\bar{q}$ bound states at $T_c < T < 4T_c$, where T_c is the transition temperature. For the physical quark mass, the QCD transition is a nonsingular crossover at finite temperature. In recent lattice results, at high temperatures and small densities, it is a crossover from the hadronic phase to QGP phase [7,8]. From recent theoretical studies, we have realized the rich phases of QCD theory, such as the color superconducting phase [9], pion condensation [10], color glass condensate, and quarkyonic phase [11]. Now the RHIC results tell us that after deconfinement, the quarks are not free immediately, as we usually thought for a weakly coupled QGP (wQGP), but are still in a strong coupled state as the sQGP. It is a challenge for us to understand this new state of nuclear matter [12]. As we know, phenomenologically, a linear confine potential and color Coulomb potential exist between quarks in vacuum, know as $V \sim \alpha/r + kr$. With temperature T increased to some critical temperature, the linear confine potential disappears, while the Coulomb potential remains, which could still be very strong [13]. Thus in the literature, the effective Coulomb potential has been often used to describe the strong interaction of sQGP [14,15]. In recent years, experiments and theories have been developing rapidly in the study of the sQGP. For new frontiers of QGP study, refer to Ref. [16].

However, in the present work, to obtain a simple and intuitive picture of sQGP, we will use a simple model to study the possible physical mechanism of the bound state in sQGP and the corresponding phase diagram of deconfinement. The model used here is the Friedberg-Lee (FL) model, which has been widely discussed in past decay studies [17–19]. It has been very successful in describing phenomenologically the static properties of hadrons and their behaviors at low energy. The model consists of quark fields interacting with a phenomenological scalar field σ. The σ field is introduced to describe the complicated nonperturbative features of QCD vacuum. It naturally gives a color confinement mechanism in QCD theory. The model has been also extended to finite temperatures and densities to study the deconfinement phase transition [20–24]. However, it seems that the deep meaning of the soliton solutions in deconfinement phase transition has not been revealed in the past studies. The main purpose of this paper is to study in detail the properties of the solitons in the FL model before and after deconfinement and provide a possible explanation and description of sQGP through this effective theoretical model.

The organization of this paper is as follows: In Sec. II we give a brief introduction of the FL model. The field equations and the effective potential are derived. In Sec. III, the soliton equation of the FL model is solved for certain boundary conditions and the physical meanings of these solitons in deconfinement are thoroughly discussed. In Sec. IV, a phase diagram of the deconfinement phase transition is given. The last section is the summary.

II. FL MODEL AND EQUATIONS

We start from the Lagrangian of the FL model,

$$\mathcal{L} = \bar{\psi}(i\gamma_\mu\partial^\mu - g\sigma)\psi + \tfrac{1}{2}(\partial_\mu\sigma)(\partial^\mu\sigma) - U(\sigma), \qquad (1)$$

where

$$U(\sigma) = \tfrac{1}{2!}a\sigma^2 + \tfrac{1}{3!}b\sigma^3 + \tfrac{1}{4!}c\sigma^4 + B. \qquad (2)$$

ψ represents the quark field, and σ denotes the phenomenological scalar field. a, b, c, g, and B are the constants which are generally fitted in with producing the properties of hadrons appropriately at zero temperature.

At finite temperature and for the thermal equilibrium system, the σ field will be replaced by $\bar{\sigma} + \sigma'$, where $\bar{\sigma}$ is the Gibbs thermal average of the σ field, and σ' is the fluctuation.

At tree level, one can obtain the field equations [22]

$$(i\gamma_\mu\partial^\mu - g\bar{\sigma})\psi = 0, \tag{3}$$

$$\partial_\mu\partial^\mu\bar{\sigma} = -\left(\frac{\partial U}{\partial\bar{\sigma}} + \frac{1}{2}(b + c\bar{\sigma})\langle\sigma'^2\rangle + g\langle\bar{\psi}\psi\rangle\right) \equiv -\frac{\partial V_{\text{eff}}}{\partial\bar{\sigma}}, \tag{4}$$

where $\langle\sigma'^2\rangle$ and $\langle\bar{\psi}\psi\rangle$ denote the contributions of the thermal excitations of σ and quark fields, respectively,

$$\langle\sigma'^2\rangle = \int \frac{d^3\mathbf{p}}{(2\pi)^3}\frac{1}{E_\sigma}\frac{1}{e^{\beta E_\sigma} - 1}, \tag{5}$$

$$\langle\bar{\psi}\psi\rangle = -\gamma\int \frac{d^3\mathbf{p}}{(2\pi)^3}\frac{m_q}{E_q}\left(\frac{1}{e^{\beta(E_q-\mu)}+1} + \frac{1}{e^{\beta(E_q+\mu)}+1}\right), \tag{6}$$

in which β is the inverse temperature, μ is the chemical potential, and γ is a degenerate factor, $\gamma = 2(\text{spin}) \times 2(\text{flavor}) \times 3(\text{color})$. $E_\sigma = \sqrt{\vec{p}^2 + m_\sigma^2}$ and $E_q = \sqrt{\vec{p}^2 + m_q^2}$; $m_q = g\bar{\sigma}$ and $m_\sigma^2 = a + b\bar{\sigma} + \frac{1}{2}c\bar{\sigma}^2$ are the effective masses of the quark and σ fields, respectively. One should notice that the second equality of Eq. (4) means that we define a thermal effective potential as

$$V_{\text{eff}} = U(\bar{\sigma}) + \frac{1}{\beta}\int\frac{d^3\mathbf{p}}{(2\pi)^3}\ln(1 - e^{-\beta E_\sigma}) - \frac{\gamma}{\beta}\int\frac{d^3\mathbf{p}}{(2\pi)^3}[\ln(1 + e^{-\beta(E_q-\mu)}) + \ln(1 + e^{-\beta(E_q+\mu)})]. \tag{7}$$

It could be seen that the V_{eff} is just the one-loop effective potential at finite temperature and density. One should notice that V_{eff} here plays dual roles at the microscopic and macroscopic levels. At the microscopic level, it acts as the effective potential within a hadron embedded in a hot and dense environment. At the macroscopic level, it plays the role of a thermodynamic function of the thermodynamic system consisting of quarks interacting with the scalar fields.

From Eq. (4), one could see that the properties of the soliton field $\bar{\sigma}$ depend completely on the effective potential V_{eff}. As known, by the effective potential at finite temperature and density, one can study the deconfinement phase transition in the FL model. Thus the properties of solitons in deconfinement, especially the relations between solitons and deconfinement, could be well studied by solving Eq. (4) at finite temperature and density.

For the model parameters a, b, c, and g, different sets of values can be chosen [23]. For the problem we discuss here, they will give similar physical results. Thus in our following calculation, we just take one set of values as $a = 17.7\ \text{fm}^{-2}$, $b = -1457.4\ \text{fm}^{-1}$, $c = 20\,000$, and $g = 12.16$, which has been often used in the literatures. The effective mass of the σ field is fixed at $m_\sigma = 550$ MeV [22,23].

At zero temperature and density, the V_{eff} is just the $U(\bar{\sigma})$ and has been plotted in Fig. 1. There are two minima of the potential $U(\bar{\sigma})$: one corresponds to the perturbative vacuum at $\bar{\sigma} = 0$, another corresponds to the physical vacuum at $\bar{\sigma} = \sigma_v$.

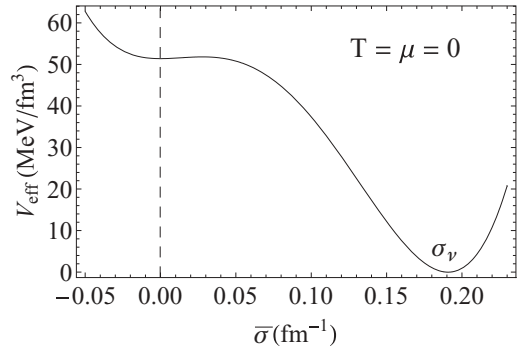

FIG. 1. Effective potential at zero temperature and density.

The difference in the potential of the two vacuum states is the bag constant B. If we take $U(\sigma_v) = 0$, the bag constant B can be expressed as

$$-B = \tfrac{1}{2!}a\sigma_v^2 + \tfrac{1}{3!}b\sigma_v^3 + \tfrac{1}{4!}c\sigma_v^4. \tag{8}$$

At finite temperature and zero chemical potential, from Eq. (7), the V_{eff} can be numerically evaluated and is plotted in Fig. 2. There are two critical temperatures T_{c1} and T_{c2}. At T_{c1}, the two minima degenerate. At T_{c2}, the minimum $\bar{\sigma} = \sigma_v$ just vanishes. The bag constant is now temperature dependent $B(T)$. For $T \leqslant T_{c1}$, it is defined as

$$B(T) = V_{\text{eff}}(\bar{\sigma} = 0; T) - V_{\text{eff}}(\bar{\sigma} = \sigma_v; T), \tag{9}$$

which can be numerically evaluated. From Fig. 2, it is easy to see that the bag constant will decrease with increasing temperature. Until at $T = T_{c1}$ the two vacuums degenerate, the bag constant is zero. There is no bag constant to provide dynamical mechanism to confine the quarks. At this time, the deconfinement phase transition occurs. For thorough discussions about the bag constant and deconfinement phase transition in the FL model, see Ref. [23].

III. SOLITON SOLUTIONS AND sQGP IN DECONFINEMENT

For the static and spherically symmetric soliton field, Eq. (4) becomes

$$\frac{d^2\bar{\sigma}}{dr^2} + \frac{2}{r}\frac{d\bar{\sigma}}{dr} = \frac{\partial V_{\text{eff}}}{\partial\bar{\sigma}}. \tag{10}$$

We will solve this equation numerically. A standard numerical package COLSYS will be used for the numerical calculation [25].

For solving the soliton equation (10), one should know the different configurations of the thermal effective potential V_{eff} and determine the boundary conditions. However, because V_{eff} is highly nonlinear in $\bar{\sigma}$ as shown in Eq. (7), it is not easy to solve the equation using COLSYS. At finite temperature and zero chemical potential, since V_{eff} can be plotted as shown in Fig. 2, we can fit every curve in terms of $\bar{\sigma}^2$, $\bar{\sigma}^3$, and $\bar{\sigma}^4$ with the effective parameters $a(T)$, $b(T)$, and $c(T)$. That means

$$V_{\text{eff}} = \tfrac{1}{2!}a(T)\bar{\sigma}^2 + \tfrac{1}{3!}b(T)\bar{\sigma}^3 + \tfrac{1}{4!}c(T)\bar{\sigma}^4 + B(T). \tag{11}$$

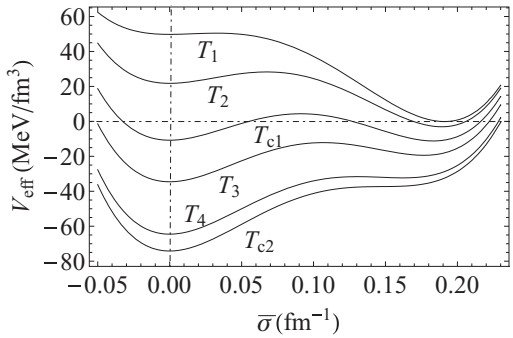

FIG. 2. Effective potentials for different temperatures and zero chemical potential: $T_1 = 50$, $T_2 = 100$, $T_{c1} = 121$, $T_3 = 130$, $T_4 = 140$, and $T_{c2} = 143$ MeV.

In this form, $V_{\rm eff}$ can be applied in COLSYS for the numerical calculation. In the following, we will solve Eq. (10) under certain boundary conditions and discuss the soliton solutions for different configurations of $V_{\rm eff}$.

At $T < T_{c1}$, the boundary condition are taken as

$$\left.\frac{d\bar{\sigma}}{dr}\right|_{r=0} = 0, \quad \bar{\sigma}|_{r\to\infty} = 0. \tag{12}$$

From Fig. 2, at $T < T_{c1}$, the physical vacuum at $\bar{\sigma} = \sigma_v$ is stable. The bag constant $B \neq 0$ and its value decreases with increasing temperature. The corresponding quarks are confined. Equation (10) can be numerically solved, and the soliton solutions are plotted in Fig. 3(a). One can see that the solitons at temperature $T < T_{c1}$ do not change so much. The quarks keep confined in a hadronic state until the critical temperature $T = T_{c1}$ at which the two vacuums degenerate. As the bag constant $B = 0$, the hadrons are destructed, and the quarks are deconfined. The corresponding soliton is also plotted in Fig. 3(a).

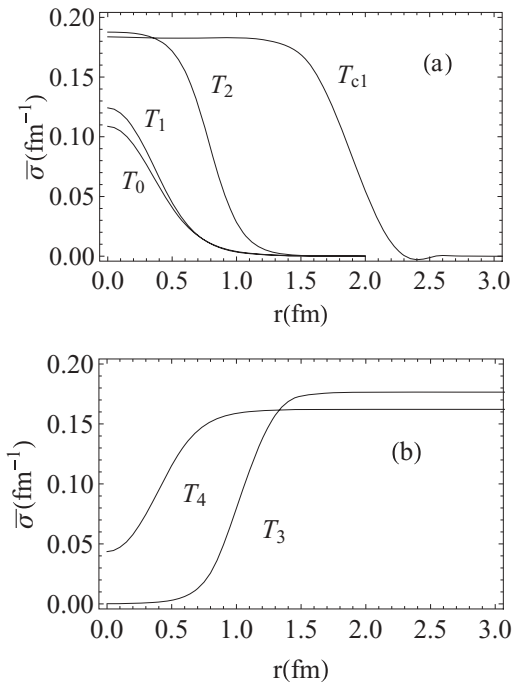

FIG. 3. Soliton solutions for different temperatures and zero chemical potential. (a) $T_0 = 0$, $T_1 = 50$, $T_2 = 100$, and $T_{c1} = 121$ MeV. (b) $T_3 = 130$ and $T_4 = 140$ MeV.

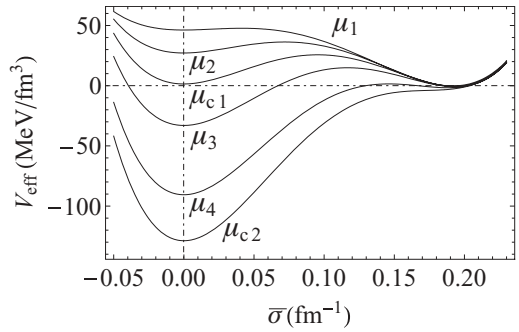

FIG. 4. Effective potentials at different chemical potentials when fixing the temperature T at 50 MeV: $\mu_1 = 100$, $\mu_2 = 200$, $\mu_{c1} = 255$, $\mu_3 = 300$, $\mu_4 = 350$, and $\mu_{c2} = 375$ MeV.

If we keep increasing temperature to $T_{c1} < T < T_{c2}$, from Fig. 2, the perturbative vacuum $\bar{\sigma} = 0$ is stable. Equation (10) will be solved under the boundary conditions

$$\left.\frac{d\bar{\sigma}}{dr}\right|_{r=0} = 0, \quad \bar{\sigma}|_{r\to\infty} = \sigma_v. \tag{13}$$

The soliton solutions are solved and plotted in Fig. 3(b). These solitons are quite different from those at $T < T_{c1}$. Since the system is already deconfined, these solitons do not represent hadrons any more but rather the bound states of quarks. Though the quarks are deconfined, they are still in strong coupled states.

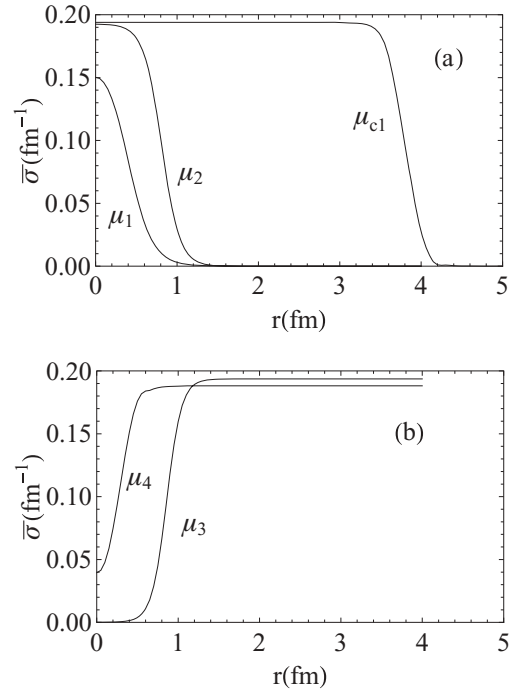

FIG. 5. Soliton solutions at different chemical potentials when fixing the temperature T at 50 MeV. (a) $\mu_1 = 100$, $\mu_2 = 200$, and $\mu_{c1} = 255$ MeV. (b) $\mu_3 = 300$ and $\mu_4 = 350$ MeV.

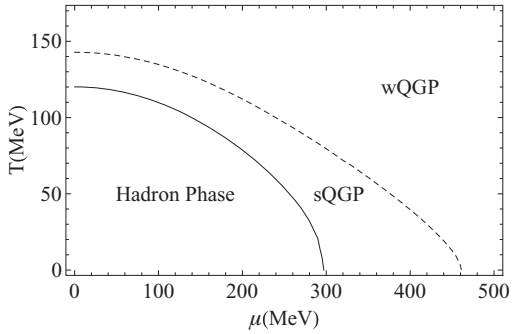

FIG. 6. Phase diagram of deconfinement in the FL soliton model.

That is, the system is in a sQGP phase. At $T = T_{c2}$, when the physical vacuum $\bar{\sigma} = \sigma_v$ vanishes and only the perturbative vacuum $\bar{\sigma} = 0$ exists, the soliton solution disappears. At this time, the quarks become quasifree, and the system goes into a quasifree gas phase of QGP, which can be identified as wQGP.

At fixed finite temperature and varying chemical potential, we can make similar observations. In Fig. 4, we show V_{eff} at $T = 50$ MeV and for different chemical potentials. There are also two critical chemicals μ_{c1} and μ_{c2}. At μ_{c1} the two vacuums degenerate; at μ_{c2} the vacuum of $\bar{\sigma} = \sigma_v$ just vanishes. The corresponding soliton solutions are plotted in Figs. 5(a) and 5(b). It is clear that at $\mu < \mu_{c1}$, the solitons representing the quarks are confined in hadronic states, and the system is in a hadronic phase. At $\mu_{c1} \leqslant \mu < \mu_{c2}$, the solitons represent bound states of quarks, and the system is in a sQGP phase. At $\mu \geqslant \mu_{c2}$, the solitons disappear. That means the quarks become quasifree and the system is in a wQGP phase.

From the above discussions, we see the physical meaning of the solitons: before deconfinement, the solitons represent hadrons; after deconfinement, the solitons represent the bound states of quarks. In the hadronic phase, the quarks are confined in a soliton bag, and the system is composed of hadrons. In the sQGP phase, the bag is destroyed, and the quarks are deconfined, but the soliton at this time can make quarks in a bound state. Thus the system is composed of clusters of quarks. In the wQGP phase, the soliton disappears, and the quarks are set free out of the bound states, and the system is composed of quasifree quarks. The solitons after deconfinement could provide a possible formation mechanism of the bound states in sQGP.

IV. PHASE DIAGRAM

Now we are in a position to plot the phase diagram of deconfinement phase transition in the FL model. When the chemical potential is fixed, one could obtain two critical temperatures. Increasing the chemical potential to another fixed value, the other two corresponding critical temperatures could be obtained, and so on. The μ-T phase diagram could be plotted as shown in Fig. 6. The full line is the dividing line between the hadronic and deconfined quark phases. The dashed line further divides the deconfined quark phase into the sQGP and wQGP phases.

V. SUMMARY

In this paper, we have thoroughly discussed the soliton solutions in the FL model at finite temperatures and densities for certain boundary conditions. The physical interpretations of the solitons in the deconfinement phase transition have been given. In the FL model, the system is deconfined at the time that the bag constant becomes zero. We indicate that the solitons before deconfinement are hadrons, while the solitons after deconfinement represent the bound states of quarks, which could possibly lead to the sQGP phase. This is very different from previous studies with the FL model, in which there is no sQGP. The whole phase diagram is divided into three phases: the hadronic, the sQGP, and the wQGP. The model and our calculation have limitations. We only calculate the one-loop effective potential which is equivalent to the mean-field treatment. At mean-field approximation, the thermodynamic contributions could not counteract the cubic term σ^3 in the effective potential. From Landau theory, the deconfinement phase transition here could only be first order. At low densities and high temperatures, there is no second-order phase transition or crossover. This is the limitation of this work. However, this model provides possibilities for further investigation of these problems. For examples, for high-temperature and low-density areas, once the nonlinear effects of the fluctuations are considered, the cubic term σ^3 may disappear in the effective potential, where the second-order phase transition may be occur. Furthermore, one could study the tunnel effects at the time the physical vacuum and perturbative vacuum degenerate, which could give a possible physical mechanism to explain the crossover. All these problems will be thoroughly studied in our future work. The QCD phase structure still needs lots of thorough investigation, especially for the finite-density areas, where the results are often model dependent. Here we only present a possible phase diagram based on the FL model, which is qualitatively consistent with that of Shuryak [1].

ACKNOWLEDGMENTS

We are thankful to Hong Mao for helpful discussions on numerical calculations. This work was supported in part by the National Natural Science Foundation of China with No. 10905018 and No. 10875050.

[1] E. V. Shuryak and I. Zahed, Phys. Rev. C **70**, 021901 (2004).
[2] M. Gyulassy and L. McLerran, Nucl. Phys. A **750**, 30 (2005).
[3] J. I. Kapusta, J. Phys. G **34**, S295 (2007).
[4] D. Teaney, J. Lauret, and E. V. Shuryak, Phys. Rev. Lett. **86**, 4783 (2001).
[5] P. F. Kolb, P. Huovinen, U. Heinz, and H. Heiselberg, Phys. Lett. B **500**, 232 (2001).
[6] D. Teaney, Phys. Rev. C **68**, 034913 (2003).
[7] Z. Fodor and S. D. Katz, J. High Energy Phys. 04 (2004) 050.

[8] F. Karsch, in *CPOD2006 Proceedings*, PoS(CPOD2007) 026 (SISSA, Trieste, Italy, 2007); in *LAT2007 Proceedings*, PoS(LAT2007) 015 (SISSA, Trieste, Italy, 2007).
[9] M. Alford, K. Rajagopal, and F. Wilczek, Phys. Lett. B **422**, 247 (1998); K. Rajagopal, Prog. Theor. Phys. Suppl. **131**, 619 (1998); R. Rapp, T. Schafer, E. V. Shuryak, and M. Velkovsky, Phys. Rev. Lett. **81**, 53 (1998).
[10] D. T. Son and M. A. Stephanov, Phys. Rev. Lett. **86**, 592 (2001); K. Splittorff, D. T. Son, and M. A. Stephanov, Phys. Rev. D **64**, 016003 (2001); J. B. Kogut and D. Toublan, *ibid.* **64**, 034007 (2001).
[11] L. D. McLerran and R. Venugopalan, Phys. Rev. D **49**, 2233 (1994); E. Iancu and L. McLerran, Phys. Lett. B **510**, 145 (2001); L. McLerran and R. Pisarski, Nucl. Phys. A **796**, 83 (2007).
[12] T. D. Lee, Nucl. Phys. A **750**, 1 (2005).
[13] K. Yagi, T. Hatsuda, and Y. Miake, *Quark-Gluon Plasma* (Cambridge University, New York, 2005).
[14] G. E. Brown, C.-H. Lee, M. Rho, and E. V. Shuryak, Nucl. Phys. A **740**, 171 (2004); E. V. Shuryak and I. Zahed, Phys. Rev. D **70**, 054507 (2004).
[15] A. Mocsy and P. Petreczky, Phys. Rev. D **77**, 014501 (2008).
[16] E. V. Shuryak, J. Phys. G **35**, 104044 (2008); Prog. Part. Nucl. Phys. **62**, 48 (2009).
[17] R. Friedberg and T. D. Lee, Phys. Rev. D **15**, 1694 (1977); **16**, 1096 (1977); **18**, 2623 (1978).
[18] R. Goldflam and L. Wilets, Phys. Rev. D **25**, 1951 (1982).
[19] M. C. Birse, Prog. Part. Nucl. Phys. **25**, 1 (1990).
[20] H. Reinhardt, B. V. Dang, and H. Schulz, Phys. Lett. B **159**, 161 (1985).
[21] M. Li, M. C. Birse, and L. Wilets, J. Phys. G **13**, 1 (1987).
[22] E. K. Wang, J. R. Li, and L. S. Liu, Phys. Rev. D **41**, 2288 (1990); S. H. Deng and J. R. Li, Phys. Lett. B **302**, 279 (1993).
[23] S. Gao, E. K. Wang, and J. R. Li, Phys. Rev. D **46**, 3211 (1992).
[24] H. Mao, R. K. Su, and W. Q. Zhao, Phys. Rev. C **74**, 055204 (2006); H. Mao, M. J. Yao, and W. Q. Zhao, *ibid.* **77**, 065205 (2008).
[25] U. Ascher, J. Christiansen, and R. D. Russell, ACM Trans. Math. Software **7**, 209 (1981).